Allylcytisine as a convenient scaffold for the construction of the π,σ-coordination compound {*Acyt*(H^+)}[Cu_8{*Acyt*(H^+)}Cl_{10}] with the unusual anionic 1*D*-coordination polymer

Yurii Slyvka[a],* Evgeny Goreshnik[b], Nazariy Pokhodylo[a], Dmitry Morozov[c], Mykola Tupychak[a], Marian Mys'kiv[a]

[a]*Ivan Franko National University of Lviv, Kyryla i Mefodiya Str., 6, 79005, Lviv, Ukraine*
[b]*Jožef Stefan Institute, Jamova 39, SI-1000 Ljubljana, Slovenia*
[c]*Nanoscience Center, Univeristy of Jyväskylä, P.O. Box 35, FI-40014 Jyväskylä, Finland*

Abstract

The aim of this work is to develop a novel π-coordination compound with unusual architecture using allylcytisine (*Acyt*) as a suitable scaffold. The synthesis and structural characterization of {*Acyt*(H^+)}[Cu_8{*Acyt*(H^+)}Cl_{10}] (**1**) and *Acyt* itself have been performed, accompanied by quantum chemical studies. A distinctive feature of structure **1** is the formation of H-bonded pairs of two {*Acyt*(H^+)} cations, showing the non-equivalent participation of its allyl group regarding to Cu^+ coordination, thus forcing the organization of the acentric structure **1** with the unusually organized anionic copper(I) halide 1*D*-coordination polymer.

***Keywords*:** Copper(I); η^2-Interaction; Cytisine; Allyl derivative; Crystal structure

1. Introduction

Cytisine is well known alkaloid from plants of the Leguminosae family (especially the seeds of *Laburnum anagyroides*), which was introduced as a smoking cessation drug due to its high affinity for nicotinic acetylcholine receptors and acting as their partial agonist [1–3]. Despite significant advances in the comprehensive studies of the biological activity of cytisine and its derivatives [4–8], the use of these compounds as co-ligands in coordination chemistry of *d*-metals remains practically unexplored. According to the Cambridge Structural Database [9], there are only four coordination compounds of such type: in copper(II) and zinc(II) compounds N-protonated cytisine is bound to the central ion by the carbonyl O atom only [10], while in an organometallic coordination compound containing palladium(II) the neutral cytisine molecule, in its bonding with the Pd(II) cation, uses another center – the most nucleophilic N atom of the amine group [11].

To support Cu^+ binding with cytisine, a nitrogen atom N(12)-modification can be used for incorporating the complexing group. The appearance of the allylic substituent on this amine N atom

* Corresponding author.
E-mail address: yurii.slyvka@lnu.edu.ua (Yu. Slyvka)

may serve as an actual key for the selected coordination of transition metal ions due to the metal-olefin π-bonding [12], forcing a significant influence on cytisine coordination capabilities. As an example, several novel allylazole ligands in its π-complexation with copper(I) were studied earlier [13–15]. The proposed concept is effective in crystal engineering of the unique π,σ-coordination compounds with unknown (or less stable) in the free state Cu^{I} salts [16,17]. Some of these copper(I)-containing compounds turned out to be very promising in obtaining advanced laser operated materials [18–20]. N-Allyl derivatives of heterocycles were also found very favourable for the construction of coordination polymers of different dimensionality as well as the cluster compounds [21–26].

In this report, to insight how the incorporation of allyl substituent to cytisine makes it a convenient scaffold for the construction of novel π,σ-coordination compounds, we described the synthesis and structural characterization of $\{Acyt(H^+)\}[Cu_8\{Acyt(H^+)\}Cl_{10}]$ (**1**) π,σ-coordination compound (*Acyt* – N12-Allylcytisine) with the unusual anionic cupro(I)chloride inorganic chain. Since the crystal structure of allylcytisine has not been studied earlier by single crystal X-ray diffraction, here we present a thorough structural analysis of *Acyt* itself.

2. Experimental section

2.1 Materials and instrumentation

Unless mentioned otherwise, all chemicals were obtained from commercial sources and used without further purification. The NMR experiments: ^{1}H NMR (500 MHz), $^{13}C\{^{1}H\}$ NMR (125 MHz) for allylcytisine *Acyt* were recorded on a Bruker Avance 500 MHz NMR spectrometer. The chemical shifts are reported in ppm relative to the residual peak of the deuterated DMSO for the ^{1}H and $^{13}C\{^{1}H\}$ NMR spectra. Raman spectra from crystals were recorded with a Horiba Jobin–Yvon LabRAM HR spectrometer with the use of the 632.81 nm excitation line of a He-Ne laser (17 mW). Diffraction data for *Acyt* and coordination compound **1** were collected on an Agilent Gemini A four-circle diffractometer with Atlas CCD detector. Quantum chemical calculations of geometry optimization and simulation of vibrational (Raman) spectra of the *Acyt* and its coordination compound **1** have been performed using GAMESS(US) quantum chemistry package [27]. Energy framework calculations were performed on the DFT/B3LYP/6-31G(d, p) level using the CrystalExplorer 17.5 software [28]**.**

2.2 Preparation of the ligand

N(12)-Allylcytisine (3-allyl-1,2,3,4,5,6-hexahydro-8*H*-1,5-methanopyrido[1,2-a][1,5]diazocin-8-one, *Acyt*) was prepared via direct alkylation of cytisine with allyl bromide (3-bromoprop-1-ene) (Scheme 1). To a solution of cytisine 1.9 g (0.01 mol) in DMF (50 mL) cooled to 0 °C, NaH 0.48 g

(0.012 mol) was added in portions and stirred at 0 °C until gas evolution. Allyl bromide 1.3 mL (0.015 mol) was added in small portions to the reaction mixture and left at room temperature for 12 hours. Then the reaction mixture was heated for 1 h at a temperature of 70 °C. The mixture was cooled to room temperature. Water (50 mL) was added and the DMF-water azeotrope was removed under reduced pressure. The concentrate was diluted with water (10 mL) and extracted with ethyl acetate (3 × 10 mL). The organic fraction was dried over Na_2SO_4, and the solvent was evaporated under reduced pressure. To the resulting residue, hexane (10 mL) was added and boiled for 5 min. The mixture was cooled, and allylcytisine was filtered off as white crystals. Yield 1.8 g, 78%; mp = 113 °C. ^{1}H NMR (500 MHz, DMSO-d_6) δ 7.29 (dd, J = 8.6, 7.2 Hz, 1H), 6.18 (d, J = 8.9 Hz, 1H), 6.04 (d, J = 6.6 Hz, 1H), 5.64 – 5.50 (m, 1H), 5.00 (d, J = 5.0 Hz, 1H), 4.98 (d, J = 15.4 Hz, 1H), 3.75 (d, J = 15.3 Hz, 1H), 3.68 (dd, J = 15.3, 6.4 Hz, 1H), 2.98 (s, 1H), 2.89 – 2.77 (m, 4H), 2.36 (s, 1H), 2.18 (t, J = 11.6 Hz, 2H), 1.77 (d, J = 12.5 Hz, 1H), 1.65 (d, J = 12.6 Hz, 1H); ^{13}C NMR (126 MHz, DMSO-d_6) δ 162.19, 152.13, 138.77, 135.04, 117.01, 115.30, 103.72, 60.19, 59.91, 59.51, 49.59, 34.52, 27.32, 25.19; MS (m/z, APCI) = 231 (M^+ + 1); Anal. calcd for $C_{14}H_{18}N_2O$: C, 73.01; H, 7.88; N, 12.16. Found: C, 73.14; H, 7.79; N, 12.07.

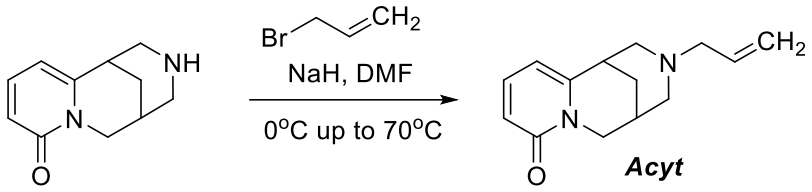

Scheme 1. The ligand *Acyt* synthesis

*2.3 Synthesis of the {Acyt(H^+)}[Cu_8{Acyt(H^+)}Cl_{10}] (**1**)*

Crystals of π,σ-coordination compound **1** were obtained under the conditions of the alternating-current electrochemical technique starting from the ethanol solution of *Acyt* and copper(II) chloride. A mixture of *Acyt* (0.66 mmol, 0.152 g) and $CuCl_2 \cdot 2H_2O$ (1.76 mmol, 0.300 g) in 5.0 mL of ethanol, acidified by two drops of 37% hydrochloric acid, was prepared and then was placed into a small 5.5 mL test-tube. Copper-wire electrodes in cork were inserted to this reactor. The alternating current (frequency 50 Hz) of 0.63 V was applied for one month, and after that the reactor was moved to the refrigerator, where it was kept at 10-11°C. After two months good quality colourless crystals of compound **1** appeared on copper-wire electrodes in a very small amount under a thin layer of white amorphous substance. M.p. 155°C.

2.3. Single crystal X-ray diffraction studies

The collected diffraction data for *Acyt* and coordination compound **1** were processed with the CrysAlis PRO program [29]. Both structures were solved by ShelXT and refined by least squares

method on F^2 using ShelXL software with the following graphical user interface of OLEX^2 [30–32]. The atomic displacement parameters for non-hydrogen atoms were refined using an anisotropic model. The amine H atoms of the *Acyt*(H^+) moieties in coordination compound **1** were derived from difference Fourier maps and refined with U_{iso}(H) = 1.2 U_{eq}(N). The other H atoms in both *Acyt* and **1** structures were refined in ideal positions (riding model), with C—H = 0.99 (methylene) or 0.95 Å (otherwise) and with U_{iso}(H) = 1.2U_{eq}(C). Crystal parameters, data collection and refinement details are summarized in Table 1. The figures were prepared using the DIAMOND 3.1 software.

Table 1. Selected crystal data and structure refinement parameters of *Acyt* and compound **1**.

Crystal data	*Acyt*	**1**
CCDC number	2173890	2173901
Empirical formula	$C_{14}H_{18}N_2O$	$C_{28}H_{38}Cl_{10}Cu_8N_4O_2$
F. w. (g·mol^{-1})	230.30	1325.44
Crystal system, space group	orthorhombic, $P2_12_12_1$	triclinic, $P1$
a (Å), α (º)	9.4309(4)	7.4509(3), 84.010(4)
b (Å), β (º)	10.7697(5)	10.7420(5), 80.982(4)
c (Å), γ (º)	11.9283(6)	12.9869(6), 81.270(4)
V (Å^3)	1211.53(10)	1011.24(8)
Z	4	1
μ (mm^{-1})	0.634	4.817
F(000)	496	652
Crystal size (mm)	0.06 × 0.21 × 0.33	0.26 × 0.35 × 0.46
Crystal color	colourless	colourless
Calculated density, g/cm^3	1.263	2.176
Data collection		
Radiation type, wavelength, λ(Å)	Cu *Ka*, 1.54184	Mo *Ka*, 0.71073
Temperature, *K*	150	150
Used in refinement reflections	2325	8664
$R[F^2 > 2\sigma(F^2)]$	0.0380	0.0375
$wR(F^2)$	0.0930	0.0852
GooF = S	1.013	1.083
Flack	0.3(5)	-0.030(13)
$\Delta\rho_{max}/\Delta\rho_{min}$ (e Å^{-3})	0.160 /-0.154	0.871/-0.792

3. Results and discussion

3.1. Crystal structure

Acyt crystallizes in the acentric space group $P2_12_12_1$, with one molecule in the asymmetric unit. Thus *Acyt* differs from earlier investigated structures of unsubstituted cytisine [33] and its benzothienopyrimidinone derivative [34], each of which has two crystallographically independent molecules. The geometry of the cytisine fragment in *Acyt* is comparable to that of unsubstituted cytisine (Fig. 1, Table 2). The allylamino group has an anticlinal conformation relative to the C12—C13 bond (N2—C12—C13—C14, –124.9(3)°). Only weak C—H···O bindings are observed among O1 center and H-donor C4, C6 & C8 atoms of nearest *Acyt* molecules.

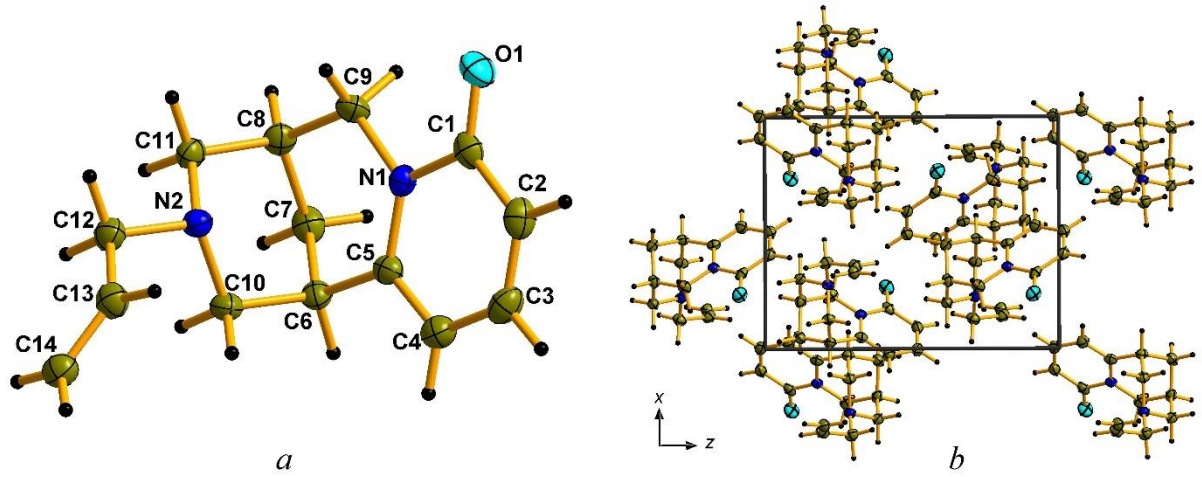

Fig. 1. *a*) The molecular structure of *Acyt* with displacement ellipsoids drawn at the 50% probability level. (*b*) A view along the *b* axis of the crystal packing of the *Acyt*.

Table 2. Selected geometric parameters (Å, º) of *Acyt* and **1**.

Acyt			
O1—C1	1.239(3)	C10—N2—C12	110.6(2)
C1—N1	1.411(3)	N2—C12—C13	112.2(2)
C13—C14	1.315(4)	C12—C13—C14	124.5(3)
Coordination compound **1**			
Cu1—Cl1	2.289(2)	Cl1—Cu1—*m*	123.4(2)
Cu1—Cl2	2.289(2)	Cl2—Cu1—*m*	121.8(2)
Cu1—Cl3	2.749(2)	Cl3—Cu1—*m*	101.6(2)
Cu1—*m*	1.963(7)	Cl1—Cu1—Cl3	102.68(7)
C13A—C14A	1.364(10)	Cl1—Cu2—Cl4	169.95(8)
Cu2—Cl1	2.133(2)	Cl3—Cu3—Cl5	158.91(9)
Cu3—Cl2	2.587(2)	Cl3—Cu3—Cl2	99.13(7)
Cu3—Cl3	2.194(2)	Cl5—Cu4—Cl2	98.18(7)
Cu4—Cl2	2.615(2)	Cl5—Cu4—Cl8^{ii}	119.62(7)
Cu5—Cl2	2.769(2)	Cl6—Cu5—Cl7	162.50(8)
Cu6—Cl7	2.288(2)	Cl2—Cu5—Cl6	95.51(7)
Cu7—Cl4^{i}	2.436(2)	Cl7—Cu6—Cl8	118.64(8)

Cu7—Cl10	2.274(2)	Cl8—Cu6—Cl9	119.87(8)
Cu3—Cu4	2.9806(15)	Cl3—Cu7—Cl10	124.37(8)
Cu5—Cu6	2.8318(14)	Cl8—Cu7—Cl10	117.77(7)
Cu6—Cu8	2.9894(14)	Cl5—Cu8—Cl9	118.55(8)
Cu3—Cu7	2.8512(14)	Cu3—Cu8—Cu6	90.09(4)
Cu3—Cu8	2.8152(14)	Cu6—Cu8—Cu7	82.17(4)
Cu7—Cu8	2.9294(14)	Cu5—Cu6—Cu8	94.80(4)

m – the mid-point of C13A=C14A bond.

Symmetry codes: (*i*) *x*+1, *y*, *z*; (*ii*) *x*−1, *y*, *z*.

Coordination compound **1** crystallizes in the acentric space group *P*1, with two *Acyt*(H^+) cations, eight Cu(I) and ten Cl ions per unit cell. One of the organic cations is π-coordinated to Cu(1) through allylic C=C bond, while the carbonyl group and the protonated amino group of this *Acyt*(H^+) are effectively involved in a symmetric N—H···O bonding with the nearest organic cation (Fig. 2, Table 3). In addition, pyrimidinone planes of the cations are also involved into π…π-stacking (centroid – centroid distance is ~3.3 Å). These cations are two conformers, which arise from the rotation of the N-allyl substituent relative to the N2—C12 bond by 102.6(8)°. The π-Bonded allylamino group has an anticlinal conformation relative to the C12A—C13A bond (N2A—C12A—C13A—C14A, –106.7(8)°), while the allylamino group of the nearest cation is characterized by an antiperiplanar conformation regarding to the analogous C12B—C13B bond (N2B—C12B—C13B—C14B, –150.7(7)°). Such extensive cationic pairs {*Acyt*(H^+)…. *Acyt*(H^+)} contribute to the formation of an unusual anionic chain.

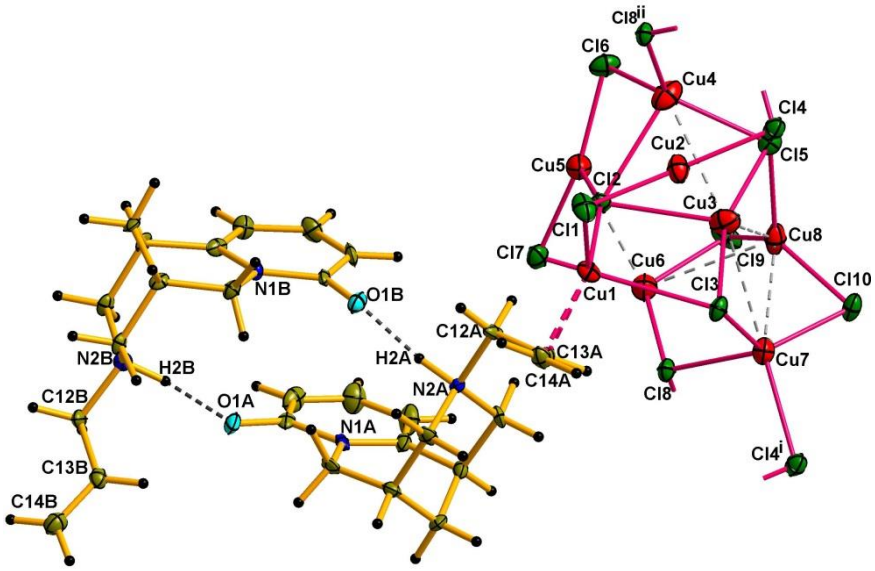

Fig. 2. The independent part in crystal structure of **1**. Displacement ellipsoids are drawn at the 50% probability level. Symmetry codes: (*i*) *x*+1, *y*, *z*; (*ii*) *x*−1, *y*, *z*.

Table 3. Hydrogen-bond geometry (Å, º) for **1**.

D—H···*A*	*D*—H	H···*A*	*D*···*A*	*D*—H···*A*
C11*B*—H11*D*···Cl4^{i}	0.99	2.83	3.709 (7)	149
N2*A*—H2*A*···O1*B*	0.97 (10)	1.71 (10)	2.667 (7)	170 (8)
N2*B*—H2*B*···O1*A*	0.96 (9)	1.71 (9)	2.652 (8)	168 (8)

Symmetry code: (*i*) *x*+1, *y*−1, *z*−1.

The π-coordinated Cu(1) cation adopts a nearly trigonal pyramidal coordination environment (3Cl, (C=C)) (Table 2). The corresponding four-coordinate geometry index τ_4 [35] for Cu(1) is 0.81. The basal plane of the coordination arrangement consists of μ_2-Cl(1), μ_4-Cl(2) ions and the η^2-allyl group. The axial site is occupied by a μ_3-Cl(3) ion at 2.749(2) Å. The π-connected to the metal centre C13A=C14A bond is elongated (due to back-donation from an occupied 3*d* metal orbital to a low-lying empty π*-orbital of the olefin) to 1.364(10) Å in comparison with uncoordinated allylic C13=C14 bond (Table 2, Fig. 3). Similarly, the Cu(4) ion has a nearly trigonal pyramidal coordination environment (4Cl, τ_4 = 0.85) with the axial μ_4-Cl(2) ion at 2.615(2) Å.

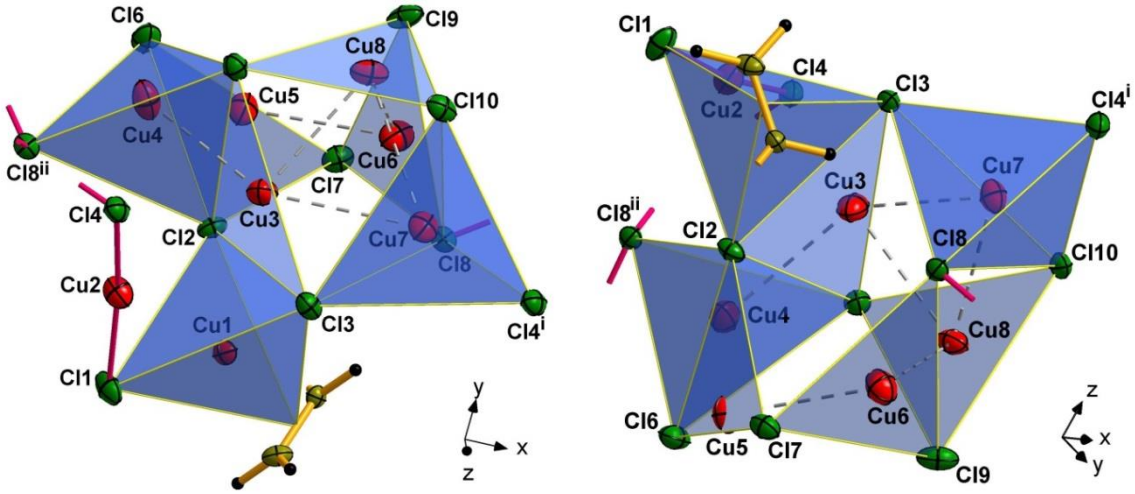

Fig. 3. A part of inorganic chain in the compound **1** at two different viewing directions and with the depicted Cu polyhedra. Symmetry codes: (*i*) *x*+1, *y*, *z*; (*ii*) *x*−1, *y*, *z*.

In the case of Cu(7), its coordination environment (τ_4 = 0.84) is formed by two μ_2-Cl and two μ_3-Cl ions, allowing Cu7 to participate in metalophilic interactions with neigboring Cu(3) and Cu(8) atoms (Cu(7)…Cu(3) 2.851(1) Å, Cu(7)…Cu(8) 2.929(1) Å). The last values are somewhat higher than the sum of the corresponding copper VdW radii (2.80 Å) published by Bondi [36] but still much smaller than the corresponding VdW radii sum obtained by Batsanov or Alvarez [37,38]. As a result, Cu(3) adopts a close to T-shaped arrangement including two closely attached to it μ_3-Cl(3) & μ_3-Cl(5) ions at 2.194(2) Å and 2.211(2) Å, correspondingly. Similar T-shaped arrangement has Cu(5), but the closest anions in its environment are μ_2-Cl(6) & μ_2-Cl(7) ions, while the third one, μ_4-Cl(2) ion is away from this metal center at 2.769(2) Å. Another closest Cu(6) and Cu(8) possess a

trigonal coordination environment. Thus, the formed clusters of Cu(3) – Cu(8) atoms defined within the anionic inorganic chain produce the specific {Cu_7{*Acyt*(H^+)}Cl_{10}} subunits (Fig. 4), which are linked by linearly-arranged Cu(2) cations and bridging μ_3-Cl(8) anions into 1*D*-polymer, extended along the *a* axis.

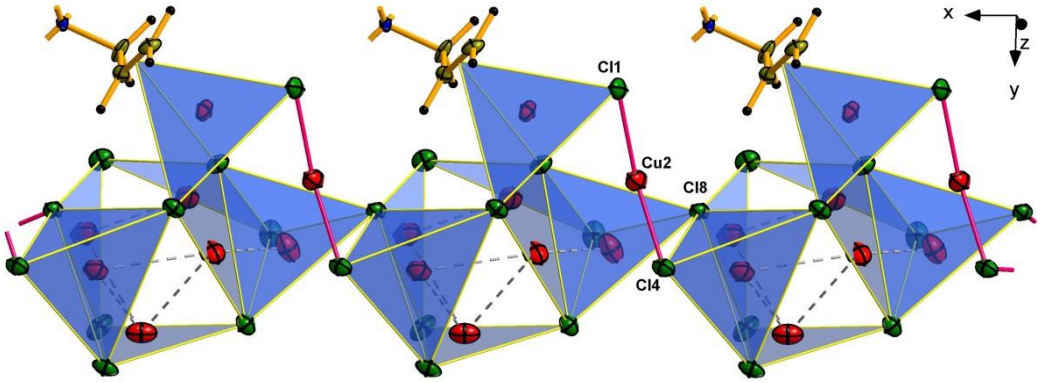

Fig. 4. Anionic inorganic chain in the compound **1** with the depicted Cu(I) polyhedra.

Most probably, the asymmetry of the above subunit and of structure **1** as a whole deals with the passivation of the allyl group of the second cation in metal binding, which in turn is enforced the by H-bond-defined location of both extensive cations (Fig. 5). This gives reason to say that the hydrogen bond between these cations competes effectively with Cu–(C=C) interaction specifying the unusual architecture of the inorganic fragment, which was impossible in the presence of allylazoles with a significant number of donor heteroatoms [12,14].

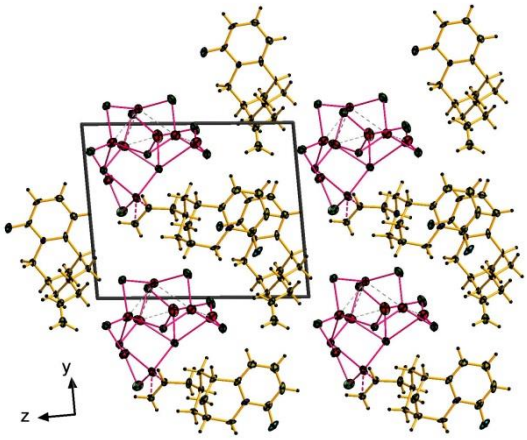

Fig. 5. A view along the *a* axis of the crystal packing of the compound **1**.

3.2. Raman spectra assignments

To simulate vibrational (Raman) spectra of the *Acyt* and its coordination compound {*Acyt*(H^+)}[Cu_8{*Acyt*(H^+)}Cl_{10}] we first have performed optimization of the bare *Acyt* (Figure 6A) and structural unit, extracted from the crystal, consisting of the two protonated *Acyt* molecules one of which forms π-coordination compound with copper(I) and 3 chloride anions ({*Acyt*(H^+)}[Cu(I){*Acyt*(H^+)}Cl_3]) shown of Figure 6. Optimizations have been performed at the

DFT level of theory using PBE0 [39] functional and aug-cc-pVDZ basis set [40] with effective core potential on Cu atom [41]. To preserve coordination from the crystal positions one Cu and three Cl atoms have been constrained during the compound optimization. After that, vibrational frequencies and corresponding Raman activities have been calculated at the optimized geometries using the same level of theory (PBE0/aug-cc-pVDZ).

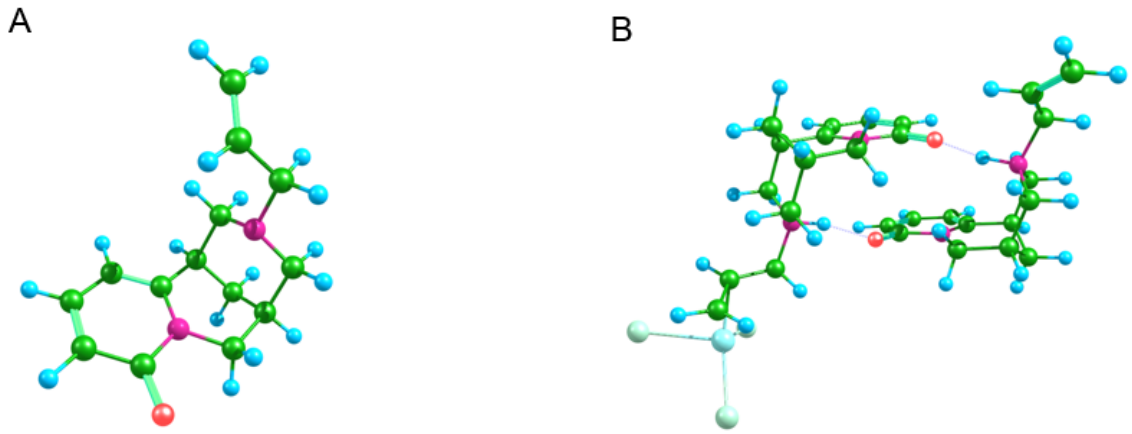

Fig. 6. Geometries of *Acyt* (panel A) and coordination compound {*Acyt*(H+)}[Cu(I){*Acyt*(H+)}Cl_3 (panel B) optimized at PBE0/aug-cc-pVDZ level of theory.

To provide ban assignments of the experimentally measured Raman spectra of the crystal, additional scaling coefficient of 0.95 have been applied to the calculated frequencies, and Raman activities have been recalculated into intensities using formalism described in the work by Michalska et.al. [42] with experimental conditions of 298K temperature and 632.81 nm (15802.53 cm^{-1}) excitation laser wavelength. In addition, spectra have been broadened with gaussian functions of 20 cm^{-1} half-width. Results of calculations and comparison between experimental and calculated spectra are shown of Figure 7A for *Acyt* molecule and Figure 7B for π-coordination compound with copper(I). Assignments of individual bands are summarized in Table 4.

As we could conclude on the basis of bare *Acyt* molecule calculations our level of theory is able to reproduce Raman spectra of studied system quiet well. Symmetric vibration of the allyl C=C bond are estimated to be around 1644 cm^{-1}. Shoulder, observed around 1652 cm^{-1} in both measured and calculated spectra corresponds to C=O vibration coupled with the symmetric ring mode. Both spectral lines at 1570 and 1545 cm^{-1} are also represent vibrational modes of the aromatic ring system.

In the large complex simulation results we could assign the same vibrational modes of the ring π-system that are coupled to the C=O vibrations around 1525 and 1590 cm^{-1}. It should be noted that C=O vibration frequency is shifted to the lower energies (1525 cm^{-1}) in comparison to the bare *Acyt* molecule (1652 cm^{-1}), which is duet too intermolecular hydrogen bonds, that present between two

Acyt molecules in the coordination compound. Moreover, we also assign vibrational bands between 1400 and 1500 cm^{-1} in the measured spectra to the bending modes of that hydrogen bonds, coupled to the ring modes. According to the simulations allyl C=C bond vibration, that forms coordination compound with Cu(I) should be also located in that region, giving us a large shift of ~180 cm^{-1} in comparison to the free C=C bond (1620 cm^{-1}) of the second *Acyt* molecule. It appears that due to strong overlap with other bands we could observe such π-complexed C=C bond vibration only as a shoulder of the peak in experimental spectra at ~1450 cm^{-1}.

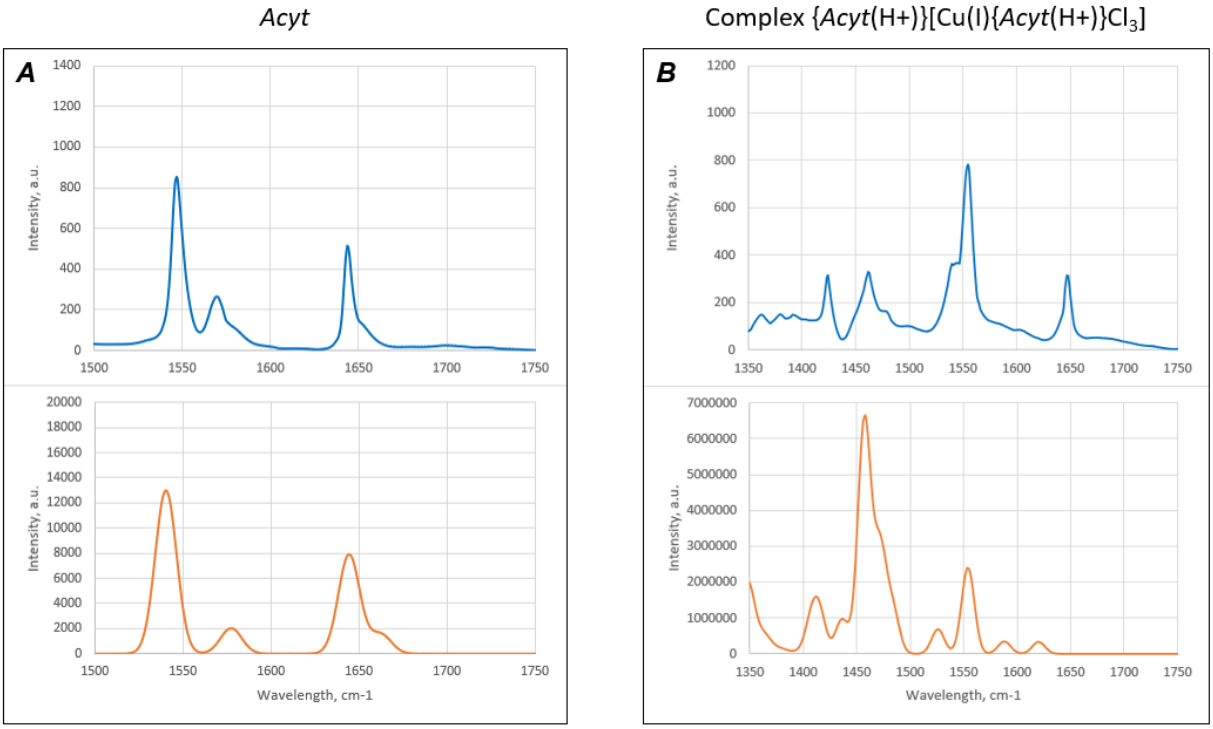

Fig. 7. Comparison of measured (upper panels) and calculated (lower panels) Raman spectra in a selected ranges of for bare *Acyt* molecule (panel A) and {*Acyt*(H+)}[Cu(I){*Acyt*(H+)}Cl_3 (panel B) coordination compound.

Table 4. Assignments of individual bands in the experimental Raman spectra of *Acyt* molecule and {*Acyt*(H^+)}[Cu_8{*Acyt*(H^+)}Cl_{10}] coordination compound.

Experimental spectra band, cm^{-1}	Assigment
Acyt	
1546	Ring π-system symmetric mode
1571, 1581 (shoulder)	Ring π-system mode coupled to C=O vibration
1644	C=C bond mode
1654 (shoulder)	C=O mode
{*Acyt*(H^+)}[Cu_8{*Acyt*(H^+)}Cl_{10}]	
1350-1400	CH_2 bending modes
1424, 1460, 1478 (shoulder)	Ring modes coupled to C=O and H-bonds bending
1450 (shoulder)	C=C π-bond to Cu(I)
1540 (shoulder), 1555	Ring π-system mode coupled to C=O vibration
1648	Free C=C bond mode

3.3. Energy framework calculations

Additionally we have performed energy frameworks computational analysis [14,28] for *Acyt* itself. All the calculations were provided for clusters of *Acyt* molecules within a radius of 3.8 Å, which were generated around a single fragment. The cylinders in the energy framework represent the relative strengths of molecular packing in different directions – interaction energies are proportional to the thickness of cylinders joining the centroids of fragments (Fig. 8).

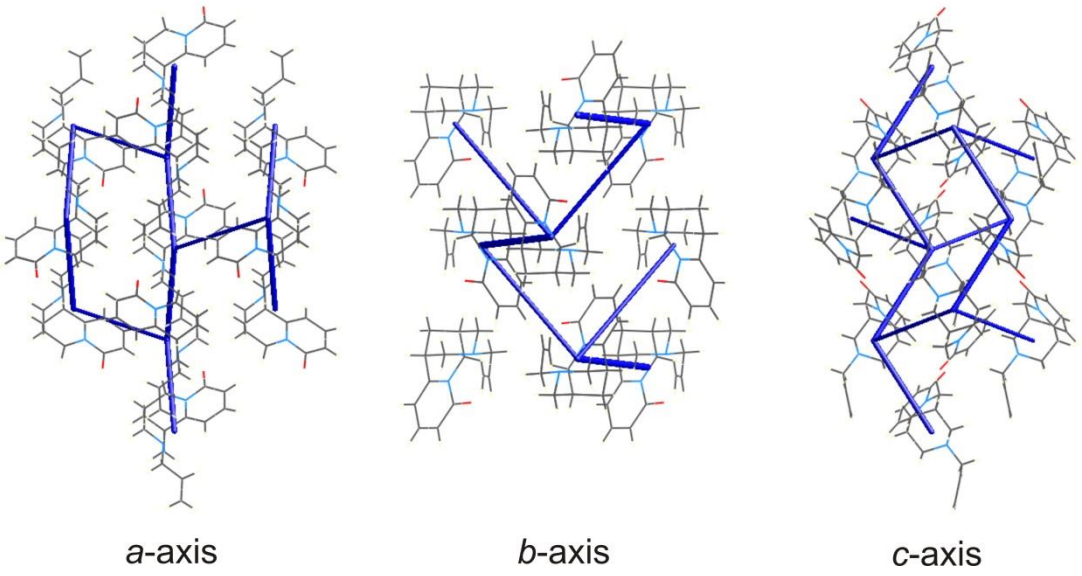

Fig. 8. Comparison energy frameworks of *Acyt* representing the total interaction energy (≤ –20 kJ/mol, blue-colored) along different crystallographic axes.

According to the calculation results the main intermolecular interactions which make the most contribution to the structure stabilization corresponds to the C—H···O hydrogen bonding between cytisine C=O group and hydrogen atoms at C4 & C6 atoms of nearest *Acyt* molecules, covering the total energy of –23.7 kJ/mol and –33.8 kJ/mol, correspondingly, with predominance of dispersive forces. Both C12—H2B···O1 bond & C11—H11···π interaction with allyl group of the same neighboring *Acyt* molecules cover the total energy of –19.3 kJ/mol and also with the predominance of dispersive forces. Next step in descending order of energy values occupy weaker C—H···O contact of –18.8 kJ/mol with C8 attached hydrogen atom, for which electrostatic and dispersion components make approximately the same contribution. The total energy of all interaction in *Acyt* structure equals –127.4 kJ/mol.

4. Conclusions

To sum up, in our work we presented how allylcytisine was used as an instrument for the construction of a novel π,σ-coordination compound {*Acyt*(H^+)}[Cu_8{*Acyt*(H^+)}Cl_{10}] (**1**) with an acentric structure. We succeeded to obtain crystals of **1** using the alternating-current

electrochemical technique and study by single crystal X-ray diffraction method. Within the unusual anionic chain in **1** there are eight crystallographically independent copper(I) ions, which form the specific $\{Cu_7\{Acyt(H^+)\}Cl_{10}\}$ subunits, linked by linearly-arranged Cu^+ cations and bridging μ_3-Cl anions into 1*D*-polymer. The design feature of the subunit is the presence of cuprophilic interactions defined by geometrically distinct coordination environments of σ-bonded copper(I) ions that possess distorted tetrahedral, closed to trigonal pyramidal, trigonal, and T-shaped arrangements. The π-coordination of the only one of two different $Acyt(H^+)$ cation to copper(I) of the anionic subunit is crucial for its formation since efficient N—H···O hydrogen bonds define the location of both extensive cations and enable second allyl group of second cation to metal binding. This gives reason to the assumption that the hydrogen bonding between these cations competes effectively with the Cu–(C=C) interaction, specifying the unusual architecture of the inorganic fragment discussed.

CRediT Authorship Contribution Statement

Yurii Slyvka: Conceptualization, Investigation, Methodology, Project administration, Software, Writing - original draft. **Evgeny Goreshnik:** Software, Investigation, Validation, Writing - original draft. **Nazariy Pokhodylo:** Software, Synthesis, Investigation, Writing - original draft. **Dmitry Morozov:** Software, Investigation, Writing - original draft. **Mykola Tupychak:** Synthesis, Investigation. **Marian Mys'kiv**: Software, Investigation.

Declaration of Competing Interest

The authors declare that they have no known competing financial interests or personal relationships that could have appeared to influence the work reported in this paper.

Acknowledgments

The authors are grateful to the Ministry of Education and Science of Ukraine (Grant Nos. 0120U101622) and the Slovenian Research Agency (ARRS) within the research program P1–0045 Inorganic Chemistry and Technology for financial support.

Appendix A. Supplementary data

CCDC 2173890 and 2173901 contain the supplementary crystallographic data for this paper. These data can be obtained free of charge from The Cambridge Crystallographic Data Centre via www.ccdc.cam.ac.uk/structures.

References

[1] N. Walker, C. Howe, M. Glover, H. McRobbie, J. Barnes, V. Nosa, V. Parag, B. Bassett, C. Bullen, Cytisine versus nicotine for smoking cessation, N. Engl. J. Med. 371 (2014) 2353–2362. doi:10.1056/NEJMoa1407764.

[2] A.E.M. Blom, H.R. Campello, H.A. Lester, T. Gallagher, D.A. Dougherty, Probing binding interactions of cytisine derivatives to the α4β2 nicotinic acetylcholine receptor, J. Am. Chem. Soc. 141 (2019) 15840–15849. doi:10.1021/jacs.9b06580.

[3] C. Gotti, F. Clementi, Cytisine and cytisine derivatives. More than smoking cessation aids, Pharmacol. Res. (2021) 105700. doi:10.1016/j.phrs.2021.105700.

[4] N. Houllier, J. Gopisetti, P. Lestage, M.-C. Lasne, J. Rouden, Identification of 9-fluoro substituted (−)-cytisine derivatives as ligands with high affinity for nicotinic receptors, Bioorg. Med. Chem. Lett. 20 (2010) 6667–6670. doi:10.1016/j.bmcl.2010.09.017.

[5] Liu, Chunming; Watt, David S.; Frasinyuk, Mykhaylo S.; Sviripa, Vitaliy M.; Zhang, Wen; and Bondarenko, Svitlana P., "Cytisine-Linked Isoflavonoid Antineoplastic Agents for the Treatment of Cancer" (2019). Markey Cancer Center Faculty Patents. 5., Application Number: 15/714,647, n.d. doi:https://uknowledge.uky.edu/markey_patents/5.

[6] M.S. Frasinyuk, W. Zhang, P. Wyrebek, T. Yu, X. Xu, V.M. Sviripa, S.P. Bondarenko, Y. Xie, H.X. Ngo, A.J. Morris, J.L. Mohler, M. V. Fiandalo, D.S. Watt, C. Liu, Developing antineoplastic agents that target peroxisomal enzymes: cytisine-linked isoflavonoids as inhibitors of hydroxysteroid 17-beta-dehydrogenase-4 (HSD17B4), Org. Biomol. Chem. 15 (2017) 7623–7629. doi:10.1039/C7OB01584D.

[7] S.P. Bondarenko, M.S. Frasinyuk, V.I. Vinogradova, V.P. Khilya, Synthesis of flavonoid derivatives of cytisine. 3. synthesis of 7-[2-(cytisin-12-yl)ethoxy]isoflavones, Chem. Nat. Compd. 48 (2013) 970–973. doi:10.1007/s10600-013-0441-3.

[8] T.-T. Peng, X.-R. Sun, R.-H. Liu, L.-X. Hua, D.-P. Cheng, B. Mao, X.-N. Li, Cytisine-pterocarpan-derived compounds: biomimetic synthesis and apoptosis-inducing activity in human breast cancer cells, Molecules. 23 (2018) 3059. doi:10.3390/molecules23123059.

[9] C.R. Groom, I.J. Bruno, M.P. Lightfoot, S.C. Ward, The Cambridge Structural Database, Acta Crystallogr. Sect. B Struct. Sci. Cryst. Eng. Mater. 72 (2016) 171–179. doi:10.1107/S2052520616003954.

[10] A.K. Przybył, M. Kubicki, R. Jastrzab, Complexing ability of (−)-cytisine — Synthesis, spectroscopy and crystal structures of the new copper and zinc complexes, J. Inorg. Biochem. 138 (2014) 47–55. doi:10.1016/j.jinorgbio.2014.04.015.

[11] S. Bouquillon, J. Rouden, J. Muzart, M.-C. Lasne, M. Hervieu, A. Leclaire, B. Tinant, Reactivity of (–)-cytisine and derivatives towards palladium salts. X-ray characterization of a

new palladium complex of (–)-cytisine, Comptes Rendus Chim. 9 (2006) 1301–1308. doi:10.1016/j.crci.2006.05.002.

[12] O.R. Hordiichuk, Yu.I. Slyvka, V. V. Kinzhybalo, E.A. Goreshnik, T.J. Bednarchuk, O. Bednarchuk, J. Jedryka, I. Kityk, M.G. Mys'kiv, Construction of heterometallic and mixed-valence copper(I/II) chloride π-complexes with 1,2,4-triazole allyl-derivative, Inorganica Chim. Acta. 495 (2019) 119012. doi:10.1016/j.ica.2019.119012.

[13] D.A. Kowalska, V. Kinzhybalo, Yu.I. Slyvka, M. Wołcyrz, Crystal structure and enantiomeric layer disorder of a copper(I) nitrate π-coordination compound, Acta Crystallogr. Sect. B Struct. Sci. Cryst. Eng. Mater. 77 (2021) 241–248. doi:10.1107/S2052520621001244.

[14] Yu. Slyvka, V. Kinzhybalo, O. Shyyka, M. Mys'kiv, Synthesis, structure and computational study of 5-[(prop-2-en-1-yl)sulfanyl]-1,3,4-thiadiazol-2-amine (Pesta) and its heterometallic π,σ-complex $[Cu_2FeCl_2(Pesta)_4[FeCl_4]$, Acta Crystallogr. Sect. C Struct. Chem. 77 (2021) 249–256. doi:10.1107/S2053229621004198.

[15] Yu.I. Slyvka, E.A. Goreshnik, N.T. Pokhodylo, M.G. Mys'kiv, $Cu(NH_2SO_3)$ π-Complexes with allyl derivatives of 1,3,4-thiadizoles: synthesis and structural formation through weak interactions, J. Chem. Crystallogr. 52 (2022) 205–213. doi:10.1007/s10870-021-00906-0.

[16] Yu. Slyvka, E. Goreshnik, O. Pavlyuk, M. Mys'kiv, Copper(I) π-complexes with allyl derivatives of heterocyclic compounds: structural survey of their crystal engineering, Open Chem. 11 (2013) 1875–1901. doi:10.2478/s11532-013-0323-3.

[17] B. Ardan, V. Kinzhybalo, Yu. Slyvka, O. Shyyka, M. Luk'yanov, T. Lis, M. Mys'kiv, Ligand-forced dimerization of copper(I)-olefin complexes bearing a 1,3,4-thiadiazole core, Acta Crystallogr. Sect. C Struct. Chem. 73 (2017) 36–46. doi:10.1107/S2053229616018751.

[18] A.A. Fedorchuk, Yu.I. Slyvka, E.A. Goreshnik, I.V. Kityk, P. Czaja, M.G. Mys'kiv, Crystal structure and NLO properties of the novel tetranuclear copper(I) chloride π-complex with 3-allyl-2-(allylimino)-1,3-thiazolidin-4-one, J. Mol. Struct. 1171 (2018) 644–649. doi:10.1016/j.molstruc.2018.06.017.

[19] A.A. Fedorchuk, Yu. Slyvka, V. Kinzhybalo, I. Kityk, J. Jedryka, K. Ozga, M. Mys`kiv, Copper(I) π-coordination compounds with allyl derivatives of disubstituted pseudothiohydantoin: synthesis, structure investigation and nonlinear optical features, J. Coord. Chem. 72 (2019) 3222–3236. doi:10.1080/00958972.2019.1687891.

[20] Yu. Slyvka, A.A. Fedorchuk, E. Goreshnik, N. Pokhodylo, J. Jedryka, K. Ozga, M. Mys'kiv, Crystal structure, DFT-study and NLO properties of the novel copper(I) nitrate π,σ-coordination compound based on 1-allyl-3-norbornan-thiourea, Polyhedron. 211 (2022) 115545. doi:10.1016/j.poly.2021.115545.

[21] Yu.I. Slyvka, A.A. Fedorchuk, N.T. Pokhodylo, T. Lis, I.V. Kityk, M.G. Mys'kiv, A novel copper(I) sulfamate π-complex based on the 5-(allylthio)-1-(3,5-dimethylphenyl)-1*H*-tetrazole ligand: Alternating-current electrochemical crystallization, DFT calculations, structural and NLO properties studies, Polyhedron. 147 (2018) 86–93. doi:10.1016/j.poly.2018.03.015.

[22] Y.-M. Song, J. Pang, K. Qian, X.-S. Wang, X.-N. Li, R.-G. Xiong, Solvothermal preparation, X-ray structural characterization and properties of two novel 3D copper(I) halide/N-allyl imidazole coordination polymers, J. Mol. Struct. 796 (2006) 210–215. doi:10.1016/j.molstruc.2006.02.050.

[23] E.A. Goreshnik, D. Schollmeyer, M.G. Mys'kiv, O. V. Pavlyuk, X-ray investigation and coordination behaviour of the 1,3-diallylbenzimidazolium cation in $[C_{13}H_{15}N_2]^+_2$ $[CuCl_{2.58}Br_{1.42}]^{2-}$ and $[C_{13}H_{15}N_2]^+[Cu_2Cl_{0.67}Br_{2.33}]^-$ complexes, Zeitschrift Für Anorg. Und Allg. Chemie. 626 (2000) 1016–1019. doi:10.1002/(SICI)1521-3749(200004)626:4<1016::AID-ZAAC1016>3.0.CO;2-Z.

[24] G. Wang, Z. Xing, L. Chen, G. Han, Two novel olefin-copper(I) coordination polymers with DHDAB as building blocks, J. Organomet. Chem. 783 (2015) 17–21. doi:10.1016/j.jorganchem.2015.01.033.

[25] E.A. Goreshnik, M.G. Mys'kiv, π-Complex of Cu(I) chloride with 1-allyloxybenzotriazole $CuCl{\cdot}C_6H_4N_3(OC_3H_5)$, Russ. J. Coord. Chem. 31 (2005) 341–346. doi:10.1007/s11173-005-0101-7.

[26] Yu.I. Slyvka, E.A. Goreshnik, B.R. Ardan, G. Veryasov, D. Morozov, M.G. Mys'kiv, A new tetranuclear copper(I) complex based on allyl(5-phenyl-1,3,4-thiadiazol-2-yl)azanide ligand: Synthesis and structural characterization, J. Mol. Struct. 1086 (2015) 125–130. doi:10.1016/j.molstruc.2015.01.010.

[27] M.W. Schmidt, K.K. Baldridge, J.A. Boatz, S.T. Elbert, M.S. Gordon, J.H. Jensen, S. Koseki, N. Matsunaga, K.A. Nguyen, S. Su, T.L. Windus, M. Dupuis, J.A. Montgomery, General atomic and molecular electronic structure system, J. Comput. Chem. 14 (1993) 1347–1363. doi:10.1002/jcc.540141112.

[28] C.F. Mackenzie, P.R. Spackman, D. Jayatilaka, M.A. Spackman, CrystalExplorer model energies and energy frameworks: extension to metal coordination compounds, organic salts, solvates and open-shell systems, IUCrJ. 4 (2017) 575–587. doi:10.1107/S205225251700848X.

[29] Rigaku, CrysAlisPro Software System, Version 1.171.41.104a. Rigaku Oxford Diffraction, http://www.rigaku.com., 2021.

[30] G.M. Sheldrick, SHELXT – Integrated space-group and crystal-structure determination, Acta

406 Crystallogr. Sect. A Found. Adv. 71 (2015) 3–8. doi:10.1107/S2053273314026370.
407 [31] G.M. Sheldrick, Crystal structure refinement with SHELXL, Acta Crystallogr. Sect. C Struct.
408 Chem. 71 (2015) 3–8. doi:10.1107/S2053229614024218.
409 [32] O. V. Dolomanov, L.J. Bourhis, R.J. Gildea, J.A.K. Howard, H. Puschmann, OLEX^2 : a
410 complete structure solution, refinement and analysis program, J. Appl. Crystallogr. 42 (2009)
411 339–341. doi:10.1107/S0021889808042726.
412 [33] P. Mascagni, M. Christodoulou, W.A. Gibbons, K. Asres, J.D. Phillipson, N. Niccolai, S.
413 Mangani, Solution and crystal structure of cytisine, a quinolizidine alkaloid, J. Chem. Soc.
414 Perkin Trans. 2. (1987) 1159. doi:10.1039/p29870001159.
415 [34] N.T. Pokhodylo, O.Y. Shyyka, Yu.I. Slyvka, E.A. Goreshnik, M.D. Obushak, Solvent-free
416 synthesis of cytisine-thienopyrimidinone conjugates via transannulation of 1*H*-tetrazoles:
417 Crystal and molecular structure, docking studies and screening for anticancer activity, J. Mol.
418 Struct. 1240 (2021) 130487. doi:10.1016/j.molstruc.2021.130487.
419 [35] L. Yang, D.R. Powell, R.P. Houser, Structural variation in copper(I) complexes with
420 pyridylmethylamide ligands: structural analysis with a new four-coordinate geometry index,
421 τ_4, Dalt. Trans. (2007) 955–964. doi:10.1039/B617136B.
422 [36] A. Bondi, van der Waals volumes and radii, J. Phys. Chem. 68 (1964) 441–451.
423 doi:10.1021/j100785a001.
424 [37] S.S. Batsanov, Van der Waals radii of elements, Inorg. Mater. 37 (2001) 871–885.
425 doi:10.1023/A:1011625728803.
426 [38] S. Alvarez, A cartography of the van der Waals territories, Dalt. Trans. 42 (2013) 8617.
427 doi:10.1039/c3dt50599e.
428 [39] C. Adamo, V. Barone, Toward reliable density functional methods without adjustable
429 parameters: The PBE0 model, J. Chem. Phys. 110 (1999) 6158–6170. doi:10.1063/1.478522.
430 [40] R.A. Kendall, T.H. Dunning, R.J. Harrison, Electron affinities of the first-row atoms
431 revisited. Systematic basis sets and wave functions, J. Chem. Phys. 96 (1992) 6796–6806.
432 doi:10.1063/1.462569.
433 [41] K.A. Peterson, C. Puzzarini, Systematically convergent basis sets for transition metals. II.
434 Pseudopotential-based correlation consistent basis sets for the group 11 (Cu, Ag, Au) and 12
435 (Zn, Cd, Hg) elements, Theor. Chem. Acc. 114 (2005) 283–296. doi:10.1007/s00214-005-
436 0681-9.
437 [42] D. Michalska, R. Wysokiński, The prediction of Raman spectra of platinum(II) anticancer
438 drugs by density functional theory, Chem. Phys. Lett. 403 (2005) 211–217.
439 doi:10.1016/j.cplett.2004.12.096.
440